Theor Chem Acc (2012) 131:1105
DOI 10.1007/s00214-012-1105-2

REGULAR ARTICLE

# Examining the impact of ancillary ligand basicity on copper(I)–ethylene binding interactions: a DFT study

**Naomi C. Pernicone · Jacob B. Geri · John T. York**

Received: 17 June 2011 / Accepted: 19 September 2011 / Published online: 5 February 2012


**Abstract** A theoretical investigation at the density functional theory level (B3LYP) has been conducted to elucidate the impact of ligand basicity on the binding interactions between ethylene and copper(I) ions in $[Cu(\eta^2\text{-}C_2H_4)]^+$ and a series of $[Cu(L)(\eta^2\text{-}C_2H_4)]^+$ complexes, where L = substituted 1,10-phenanthroline ligands. Molecular orbital analysis shows that binding in $[Cu(\eta^2\text{-}C_2H_4)]^+$ primarily involves interaction between the filled ethylene $\pi$-bonding orbital and the empty Cu(4*s*) and Cu(4*p*) orbitals, with less interaction observed between the low energy Cu(3*d*) orbitals and the empty ethylene $\pi$*-orbital. The presence of electron-donating ligands in the $[Cu(L)(\eta^2\text{-}C_2H_4)]^+$ complexes destabilizes the predominantly Cu(3*d*)-character filled frontier orbital of the $[Cu(L)]^+$ fragment, promoting better overlap with the vacant ethylene $\pi$*-orbital and increasing Cu → ethylene $\pi$-backbonding. Moreover, the energy of the filled $[Cu(L)]^+$ frontier orbital and mixing with the ethylene $\pi$*-orbital increase with increasing p$K_a$ of the 1,10-phenanthroline ligand. Natural bond orbital analysis reveals an increase in Cu → ethylene electron donation with addition of ligands to $[Cu(\eta^2\text{-}C_2H_4)]^+$ and an increase in backbonding with increasing ligand p$K_a$ in the $[Cu(L)(\eta^2\text{-}C_2H_4)]^+$ complexes. Energy decomposition analysis (ALMO-EDA) calculations show that, while Cu → ethylene charge transfer (CT) increases with more basic ligands, ethylene → Cu CT and non-CT frozen density and polarization effects become less favorable, yielding little change in copper(I)–ethylene binding energy with ligand p$K_a$. ALMO-EDA calculations on related $[Cu(L)(NCCH_3)]^+$ complexes and calculated free energy changes for the displacement of acetonitrile by ethylene reveal a direct correlation between increasing ligand p$K_a$ and the favorability of ethylene binding, consistent with experimental observations.

**Keywords** Density functional theory · Copper · Ethylene · Organometallic

## 1 Introduction

The binding of alkenes to copper(I) ions is an important step in a wide variety of chemical systems. In nature, the reversible formation of a copper(I)–ethylene adduct in the ETR 1 plant protein is a critical step in the regulation of plant growth and development [1, 2]. Synthetic processes like alkene cyclopropanation [3] and aziridination [4] are also proposed to involve the formation of labile copper(I)–alkene adducts as either resting or pre-equilibrium states in the catalytic cycles. Because the copper–alkene bonding in these complexes is generally weak and the formation of such adducts reversible, materials containing copper(I) ions are also receiving attention for use in applications that can take advantage of this reversible binding. For example, copper(I) compounds may be useful as adsorbents for the selective separation of alkenes from crude organic feedstocks [5] or as molecular sensors for detecting the presence of alkenes or other small molecules [6]. In these types of systems, the strength of the copper(I)–alkene bond may play an important role the reactivity observed, and the potential ability to tune the strength of the copper–alkene bond could be particularly useful in the rational design of

**Electronic supplementary material** The online version of this article (doi:10.1007/s00214-012-1105-2) contains supplementary material, which is available to authorized users.

N. C. Pernicone · J. B. Geri · J. T. York (✉)
Department of Chemistry, Stetson University, DeLand, FL 32723, USA
e-mail: jyork@stetson.edu

synthetic materials. Thus, understanding the different factors that impact the nature and strength of copper(I)–alkene bonds is an important goal.

Computational methods have been widely used to provide insight into the fundamental nature of copper(I)–alkene bonding [3, 4, 7–11], particularly between the simple alkene ethylene and the bare copper(I) cation in $[Cu(\eta^2\text{-}C_2H_4)]^+$ (**1**) [7–10]. Studies employing population analysis and energy decomposition analysis methods have shown that copper(I)–ethylene bonding in **1** consists of both covalent and electrostatic components [7–10], with each component providing an important contribution to the bonding stabilization. The covalent interactions are typically described using the Dewar–Chatt–Duncanson model [12] in which the two main contributions are $\sigma$-donation from the filled $\pi$-orbital of ethylene into empty frontier orbitals on the copper, and $\pi$-donation from filled copper *d*-orbitals into the empty $\pi^*$-orbital of ethylene. These theoretical studies have further concluded that ethylene → copper(I) $\sigma$-donation is the dominant covalent interaction in **1**, providing roughly 60% of the charge transfer (CT) while copper(I) → ethylene $\pi$-backbonding provides the remaining contribution [7–10].

While these investigations have yielded important insight into the bonding in **1**, copper(I)–ethylene adducts are generally stabilized by the presence of a Lewis basic ancillary ligand (L) on the copper center in synthetic systems, or by amino acid residues like histidine or cysteine in nature. A number of synthetic $[Cu(L)(\eta^2\text{-}C_2H_4)]^{n+}$ ($n = 0$, 1) complexes have been isolated or characterized using a wide variety of supporting ligands [13], with some examples including thioethers [14], tertiary amines [15], 1,10-phenanthrolines [16, 17], bipyridines [16], tris(pyrazolyl) borates [18–20], $\beta$-diketiminates [21], and iminophosphanamides [22]. In these synthetic complexes, variation in ligand donor strength is commonly purported to have an important effect, particularly on the degree of Cu → ethylene $\pi$-backbonding and, in some instances, the overall stability of the complexes themselves [13–22]. This ancillary ligand impact on the ability of copper(I) to interact with a secondary ligand has also been reported for other $[Cu(L)(X)]^{n+}$ complexes, such as those having a bidentate oxygen donor ligand [23] or CO [24, 25] as the secondary ligand "X".

Despite such reports, the full impact of ligand basicity on copper(I)–ethylene bonding is still not completely understood. Some studies have investigated the impact of ligand basicity on bonding in copper(I)–alkene and copper(I)–alkyne complexes [26–28]; however, variations in important factors including alkene identity, ligand denticity, ligand charge and ligand steric bulk complicate a direct evaluation of ligand electronic effects in significantly different $[Cu(L)(\eta^2\text{-alkene})]^{n+}$ systems. Moreover, while copper(I) → ethylene $\pi$-backbonding has been shown to play an important role in these systems, the impact of ligand basicity on additional bonding components including ethylene → Cu(I) $\sigma$-donation and non-CT effects has not been fully explored. Thus, a more comprehensive examination of copper(I)–ethylene bonding and the direct influence of ligand basicity on the different components of the interaction is warranted.

One synthetic system that provides an excellent opportunity to more clearly elucidate the electronic impact of ancillary ligand basicity on the various components of copper(I)–ethylene bonding is the series of $[Cu(L)(\eta^2\text{-}C_2H_4)]^+$ complexes originally reported by Munakata and coworkers [16, 17], where L = 1,10-phenanthroline (phen) and its derivatives (Fig. 1). The ligands in this set of compounds possess similar steric properties yet have gradually varying basicities resulting from the phenanthroline substituents, thereby allowing for clearer elucidation of the impact of ligand electron-donating ability on the copper(I)–ethylene interaction. Indeed, a ligand electronic effect was originally proposed by Munakata to explain the linear correlation observed between ligand $pK_a$ and the formation constant of $[Cu(L)(\eta^2\text{-}C_2H_4)]^+$ from free ethylene and $[Cu(L)(NCCH_3)_n]^+$ [16]. Given the widespread synthetic use of this ligand system and an experimentally demonstrated correlation between ligand basicity and ethylene binding, this system is ideal for a more comprehensive exploration of ligand electronic effects.

Presented herein are the results of a computational (DFT) investigation exploring the impact of ligand basicity on the various components of copper(I)–ethylene bonding in $[Cu(L)(\eta^2\text{-}C_2H_4)]^+$ complexes having a series of substituted 1,10-phenanthroline (phen) ligands. Bonding is first discussed in terms of a molecular orbital description obtained using the fragment molecular orbital overlap method of Gorelsky and coworkers [29, 30] as

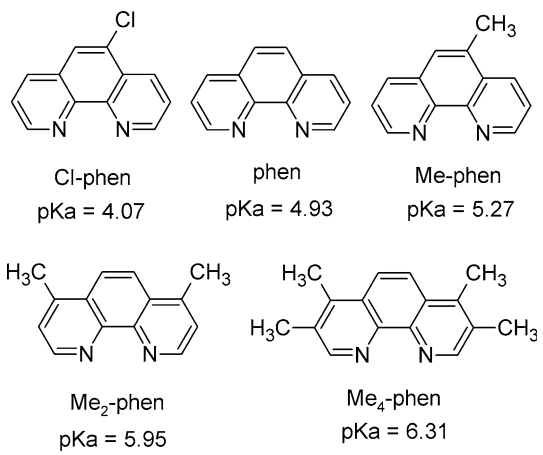


**Fig. 1** Ligands used in the calculations for $[Cu(L)(\eta^2\text{-}C_2H_4)]^+$ complexes ($pK_a$ given for $LH^+$ [16, 24])

implemented in *AOMix*. Next, the natural population and natural bond orbital (NBO) analysis method of Weinhold and coworkers [31] is employed to quantify the impact of ligand basicity on the traditional Dewar–Chatt–Duncanson components of copper(I)–ethylene bonding, including both Cu(I) → ethylene $\pi$-backbonding and ethylene → Cu(I) $\sigma$-donation. Finally, the absolutely localized molecular orbital-energy decomposition analysis (ALMO-EDA) method of Khaliullin and coworkers [32, 33] is used to quantify the impact of ligand basicity on the various contributions to copper(I)–ethylene binding energies. These results provide important insight into the fundamental nature of copper(I)–ethylene bonding, and the role ligand basicity may play in copper–alkene bonding in both synthetic and biological systems.

## 2 Computational details

All DFT calculations were performed as spin-restricted calculations using the hybrid B3LYP functional [34–36] and tight SCF convergence criteria. Geometry optimizations, analytical frequency calculations, and single-point energy calculations were performed with the Gaussian 03W [37] suite of programs (Revision E.01). Geometry optimizations for all reported structures were performed in the gas phase without symmetry constraints using tight convergence criteria, with the Stuttgart/Dresden (SDD) effective core potential and basis set [38] used for copper and the 6-31G(*d*,*p*) basis set [39, 40] used for C, H, N, and Cl atoms. All optimized structures were verified as energetic minima by the absence of imaginary frequencies in subsequent vibrational frequency calculations. Similar computational methodologies have been used successfully to model both the geometries and the binding energies of small molecules to other N-donor ligated copper(I) complexes [3, 4, 11, 25, 26, 41, 42]. Single-point energy calculations for the natural population and NBO analyses [31] were performed on optimized geometries using the SDD effective core potential and basis set for copper and the 6-311G(2*d*,*p*) basis set [43] for C, H, N, and Cl atoms. Compositions of molecular orbitals and the overlap populations between molecular fragments were calculated using the *AOMix* program (Rev. 6.51) [29, 30] with the SDD basis set and effective core potential for copper and the 6-311G(2*d*,*p*) basis set for all other atoms. Absolutely localized molecular orbital-energy decomposition analysis (ALMO-EDA) calculations were performed on the optimized structures using the method of Khaliullin and coworkers [32, 33] as implemented in Q-Chem (version 3.2) at the B3LYP level of theory using the Stuttgart-Bonn SRSC [38] effective core potential and basis set for copper and the 6-311G(2*d*,*p*) basis set for C, H, N, and Cl atoms. The default Q-Chem standard quadrature grid size (SG-1) was modified to a finer grid size of (70,302) to minimize DFT grid superposition errors. Single-point energy calculations for the determination of reaction free energy changes were performed on optimized geometries in Gaussian 03W using the SDD effective core potential and basis set for copper and the 6-311+G(2*d*,*p*) basis set [43] for C, H, N, and Cl atoms. Single-point solvation energies were computed using the CPCM solvation model [44] as implemented in Gaussian 03W with methanol as the solvent and using the 6-311+G(2*d*,*p*) basis set [43] for C, H, N, and Cl atoms and the SDD basis set for Cu. All single-point electronic energies were corrected to Gibbs free energies at 298.15 K and 1 atm using the unscaled frequencies obtained from the original frequency calculations with the SDD/6-31G(d,p) basis set combination. Reported vibrational frequencies have been scaled by 0.961 [45]. The effects of non-coordinating $ClO_4^-$ counterions present in the experimental systems were not explored in this investigation [16, 17].

## 3 Results and discussion

### 3.1 Calculated structures of copper(I)–ethylene complexes

The relevant geometric parameters for the geometry optimized structures of the $[Cu(\eta^2\text{-}C_2H_4)]^+$ cation (**1**) and $[Cu(L)(\eta^2\text{-}C_2H_4)]^+$ complexes [where L = Cl-phen (**2**), phen (**3**), Me-phen (**4**), $Me_2$-phen (**5**), and $Me_4$-phen (**6**)] are listed in Table 1. To facilitate a more thorough assessment of ligand effects on copper(I)–ethylene bonding, the structure of **1** was first explored. An examination of the calculated structure of **1** reveals a C=C bond length of 1.378 Å and Cu–C bonds of 2.107 Å. Previous computational studies of **1** by Frenking and coworkers [9] at both the MP2 level of theory (C=C, 1.378 Å; Cu–C, 2.095 Å) and the DFT level of theory [10] (BP86) (C=C, 1.390 Å; Cu–C, 2.032 Å), as well as Hertwig et al. [8] at the DFT level of theory (B3LYP) (C=C, 1.370 Å; Cu–C, 2.098 Å) yielded similar geometries. Notably, the optimized C=C distance of 1.378 Å in **1** is ~0.048 Å longer than that for free ethylene ($C{=}C_{calc}$, 1.330 Å;[1] (C=C, 1.3369(16) Å [46]).

The geometry optimized structure of the representative complex $[Cu(phen)(\eta^2\text{-}C_2H_4)]^+$ (**3**) is shown in Fig. 2, and the geometric parameters in Table 1 can be compared with the experimental X-ray structural data for $[Cu(phen)(\eta^2\text{-}C_2H_4)]ClO_4$ (**7**) [17]. Consistent with the experimental

[1] Calculated at the RB3LYP/6-31g(*d*,*p*) level of theory.

**Table 1** Selected geometric parameters for of $[Cu(L)(\eta^2\text{-}C_2H_4)]^+$ complexes **1**–**7** (all bond lengths in Å, angles in deg)

Structural data for **7** from Ref. [16]

| | **1** | **2** | **3** | **4** | **5** | **6** | **7** |
|---|---|---|---|---|---|---|---|
| C=C | 1.3778 | 1.3798 | 1.3801 | 1.3803 | 1.3810 | 1.3812 | 1.361(22) |
| Cu–N | NA | 2.043, 2.040 | 2.041 | 2.041, 2.036 | 2.031 | 2.044 | 2.002(8), 2.004(9) |
| Cu–C | 2.109 | 2.050, 2.050 | 2.050 | 2.050, 2.050 | 2.045 | 2.031 | 1.998(13), 2.022(12) |
| C–Cu–C | 39.189 | 39.336 | 39.357 | 39.386 | 39.468 | 39.503 | 39.6(6) |
| N–Cu–N | NA | 83.046 | 83.278 | 83.199 | 82.974 | 83.134 | 85.6(3) |

structure, the computed geometry of **3** contains the ethylene molecule coordinated in an $\eta^2$-fashion in the plane of the 1,10-phenanthroline ligand. The calculated Cu–N (2.041 Å), Cu–C (2.050 Å), and C=C (1.380 Å) bond lengths in **3** are in reasonable agreement with those in **7** (Cu–N, 2.002(8) Å, 2.004(9) Å; Cu–C, 1.998(13) Å, 2.022(12) Å; C=C, 1.361(22) Å). Moreover, the calculated $\nu_{C=C}$ for the coordinated ethylene molecule in **3** is 1,527 $cm^{-1}$, in excellent agreement with the experimental value of 1,525 $cm^{-1}$ measured for **7** [16, 45].

The predicted structural impact of adding an auxiliary ligand to the bare copper(I) center in **1** can be seen by comparing the optimized geometries of **1** and **3**. The calculated C=C bond length in **3** is similar to that in the unligated **1** (1.380 vs. 1.378 Å), despite the coordination of the electron-donating 1,10-phenanthroline ligand in **3**. A similar comparison of the structures of **2**–**6** (Table 1) reveals that increasing ligand $pK_a$ from 4.07 in complex **2** to 6.31 in complex **6** results in a small but consistent increase in the calculated ethylene C=C bond length ($\sim$0.0014 Å) across the series. Thus, for the $pK_a$ range in this series of copper(I) complexes, ligand basicity is predicted to directly impact the length of the ethylene C=C bond, but to a degree that would not likely be observable using typical experimental structural characterization techniques like X-ray crystallography. This is consistent with X-ray crystallographic data showing that even more strongly donating ligands like *N*,*N*,*N*′,*N*′-tetramethylethylenediamine [15], anionic $\beta$-diketiminates [21], and anionic iminophosphanamides [22] yield copper(I)–ethylene adducts having C=C bond lengths (1.36(1), 1.365(3), and 1.362(6) Å, respectively) that are similar to that in **7** (1.361(22) Å). Thus, as previously noted [5, 13], while ancillary ligand basicity is often proposed to impact the $\pi$-backbonding ability of the copper ion, the impact on the C=C bond length is small.

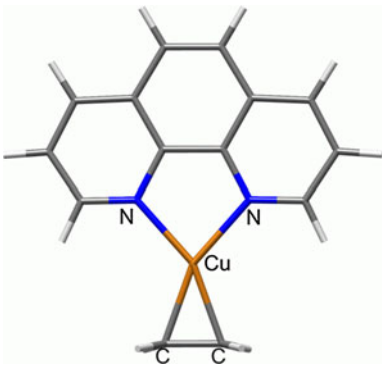


**Fig. 2** Optimized geometry of $[Cu(phen)(\eta^2\text{-}C_2H_4)]^+$

Because the length of the C=C bond is sometimes used as a measure of a metal's $\pi$-backbonding ability in metal–alkene complexes, structural data from synthetic complexes have been used to suggest that the copper(I) ion, even when coordinated by strongly electron-donating ligands, has a limited ability to $\pi$-backbond [5, 13]. Indeed, while the C=C bond is lengthened for copper(I)–ethylene adducts, it is somewhat shorter than those observed for ethylene complexes of other $d^{10}$ metals that are generally considered to be more effective at $\pi$-backbonding. Examples of these include $Pt(PPh_3)_2(\eta^2\text{-}C_2H_4)$ (1.43 Å) [47, 48] and $Ni(PPh_3)_2(\eta^2\text{-}C_2H_4)$ (1.391 Å) [49]; however, it is worth noting that, even in these complexes, the ethylene C=C bond is only lengthened by $\sim$0.1 and 0.06 Å, respectively. Because C=C bond lengthening is dependent not only on population of the ethylene $\pi$*-orbital through backbonding from the metal center but also on the depletion of electron density in the ethylene $\pi$-bonding orbital through $\sigma$-donation to empty metal orbitals [5, 13], a comprehensive analysis of the C=C bond lengths in $[Cu(L)(\eta^2\text{-}C_2H_4)]^{n+}$ complexes and its dependence on ligand basicity including the combined effect of all binding interactions is discussed below.

### 3.2 Molecular orbital analysis

Molecular orbital (MO) compositions for **1**–**6** were determined using the *AOMix* program [29, 30], and an analysis of these compositions in terms of the interaction of discrete molecular fragments was subsequently completed using the *AOMix-CDA* program [29, 30]. In this study, the molecular fragments of interest in **2**–**6** are the $[Cu(L)]^+$ cations and the ethylene molecule (for **1**, the fragments are the bare copper(I) cation and the ethylene molecule). First examining **1**, Fig. 3 shows selected molecular orbitals along with the "parent" fragment orbitals from the copper(I) ion and the ethylene molecule (Table 2). To discuss the bonding within the traditional Dewar–Chatt–Duncanson model, we first examine the interaction of the filled orbitals on the coper(I) center and empty $\pi$*-orbital on the ethylene

molecule in terms of traditional Cu → ethylene backbonding. The filled Cu(3*d*) orbitals are low in energy (−15.7 eV) compared to the vacant $\pi$*-LUFO (lowest unoccupied fragment orbital, where the term fragment orbital is used to distinguish orbitals on individual fragments from those of the complex) of the ethylene molecule (−0.2 eV). Interaction of these orbitals yields two primary molecular orbitals in **1**: the HOMO-4 [4% ethylene $\pi$*-LUFO; 94% Cu(3*d*)] and the LUMO + 1 [71% ethylene $\pi$*-LUFO; 4% Cu(3*d*); 26% Cu(4*p*)]. The small contribution of the ethylene $\pi$*-LUFO to the HOMO-4 and the similarly low contribution of the Cu(3*d*) orbitals to the LUMO + 1 are consistent with a low degree of Cu → ethylene backbonding in **1** [51, 52].

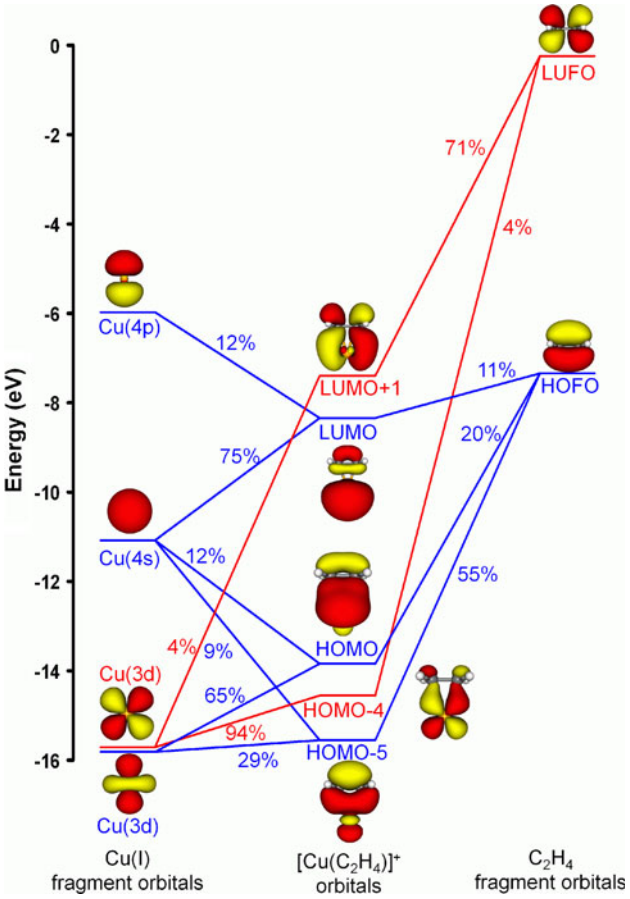


**Fig. 3** Molecular orbital interaction diagram for $[Cu(\eta^2\text{-}C_2H_4)]^+$ (only selected orbitals are shown for clarity)

**Table 2** Energy (eV) and composition (%) of $[Cu(L)]^+$ HOFO for complexes **1**–**6**

| | **1** | **2** | **3** | **4** | **5** | **6** |
|---|---|---|---|---|---|---|
| Energy | −15.72 | −10.14 | −10.03 | −9.94 | −9.77 | −9.61 |
| % Cu(3*d*) | 100 | 67 | 66 | 66 | 65 | 64 |
| % N | NA | 21 | 21 | 21 | 21 | 22 |

Similarly, the interactions between the filled $\pi$-HOFO (highest occupied fragment orbital) of the ethylene molecule and the vacant orbitals on the copper(I) center can be analyzed in terms of ethylene → Cu $\sigma$-donation. The vacant Cu(4*s*) and Cu(4*p*) acceptor orbitals lie at −11.1 and −6.0 eV, respectively, compared to the energy of the filled ethylene $\pi$-HOFO at −7.3 eV. Three primary molecular orbitals in **1** are formed from the interaction of these orbitals in what can be interpreted as traditional ethylene → Cu donation: the HOMO-5 [55% ethylene $\pi$-HOFO; 29% Cu(3*d*); 9% Cu(4*s*)], the HOMO [20% ethylene $\pi$-HOFO; 65% Cu(3*d*); 12% Cu(4*s*)], and the LUMO [11% ethylene $\pi$-HOFO; 75% Cu(4*s*); 12% Cu(4*p*)].

Molecular orbital descriptions were similarly obtained for $[Cu(L)(\eta^2\text{-}C_2H_4)]^+$ complexes **2**–**6**. The major interfragment orbital interactions are also consistent with the traditional Dewar–Chatt–Duncanson model of bonding, and selected orbital interactions for the representative complex **3** are shown in Fig. 4. The Cu → ethylene backbonding is primarily observed in the interaction of the filled $[Cu(phen)]^+$ HOFO (66% Cu(3*d*); 21% N) with the $\pi$*-LUFO of the ethylene molecule yielding the HOMO-1 (86% $[Cu(phen)]^+$ HOFO; 11% ethylene $\pi$*-LUFO) and the LUMO + 3 (8% $[Cu(phen)]^+$ HOFO; 70% ethylene

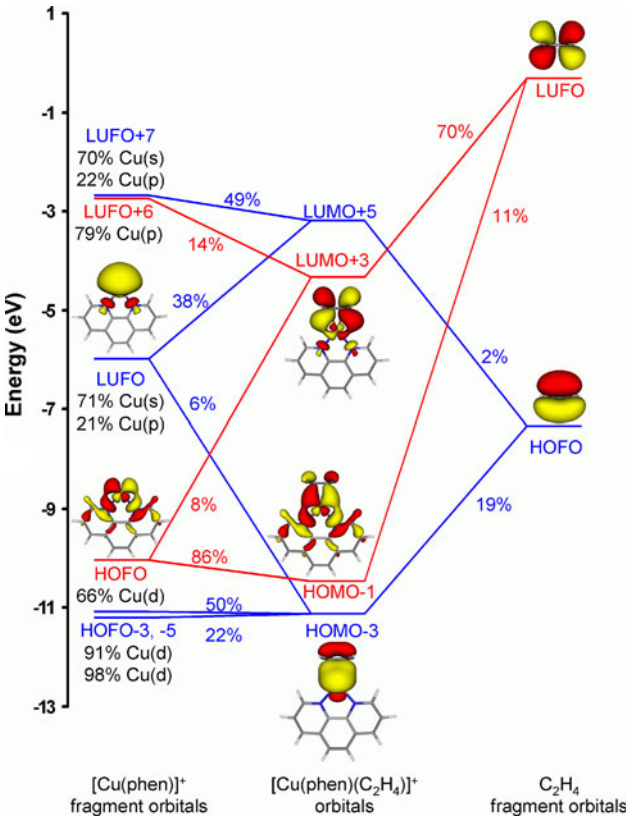


**Fig. 4** Molecular orbital interaction diagram for $[Cu(phen)(\eta^2\text{-}C_2H_4)]^+$ (only selected orbitals are shown for clarity)

$\pi$*-LUFO; 14% $[Cu(phen)]^+$ LUFO + 6) of **3**. The ethylene → Cu donation is also evidenced primarily by the interaction of the filled ethylene $\pi$-HOFO and the vacant $[Cu(phen)]^+$ LUFO [71% Cu(4*s*); 21% Cu(4*p*)] to form the HOMO-3 (19% ethylene $\pi$-HOFO; 6% $[Cu(phen)]^+$ LUFO) and HOMO-9 (35% ethylene $\pi$-HOFO; 4% $[Cu(phen)]^+$ LUFO) of **3**.

Comparing the interactions in **3** and **1**, the energy of filled HOFO of the $[Cu(phen)]^+$ fragment (−10.0 eV) in **3** is significantly higher than the pure Cu(3*d*) orbitals of **1** (−15.7 eV). Thus, as suggested previously [21, 22, 26–28], contributions from the Lewis basic N-donor ligand effectively destabilize the filled Cu(3*d*) orbitals, resulting in greater interaction with the empty ethylene $\pi$*-orbital in **3** (86% $[Cu(phen)]^+$; 11% ethylene $\pi$*-LUFO) when compared to **1** (94% Cu(3*d*); 4% ethylene $\pi$*-LUFO). This is consistent with an overall increase in Cu → ethylene backbonding in the presence of the electron-donating 1,10-phenanthroline ligand. Moreover, the energy of the HOFO of the $[Cu(L)]^+$ fragments steadily increases from **2** to **6** by ∼0.5 eV with increasing ligand basicity (Table 2). This increase in energy of the donor HOFO is accompanied by an increase in mixing between this orbital and the empty $\pi$*-LUFO of the ethylene fragment (Table 3). Thus, in this series of complexes, ligand basicity directly impacts both the energy of the $[Cu(L)]^+$ donor orbital and the amount of Cu → ethylene backbonding observed [50, 51].

### 3.3 Natural bond brbital (NBO) analysis

To further quantify the impact of ligand basicity on the magnitude of the Cu → ethylene $\pi$-backbonding and ethylene → Cu $\sigma$-donation in complexes **1**–**6**, the natural population and NBO analysis method of Weinhold and coworkers [31] was used. Because NBOs describe the molecular wavefunction in terms of orbitals that are localized on a single atom or shared by a pair of atoms [31], NBOs are useful for visualizing copper(I)–ethylene bonding in terms of the Dewar–Chatt–Duncanson model.

**Table 3** Composition of primary bonding molecular orbital resulting from the interaction of the filled $[Cu(L)]^+$ HOFO and the empty ethylene($\pi$*) LUFO in complexes **1**–**6**

| | **1** | **2** | **3** | **4** | **5** | **6** |
|---|---|---|---|---|---|---|
| % $[Cu(L)]^+$ HOFO | 94.28 | 86.58 | 86.40 | 86.24 | 85.91 | 85.70 |
| % $C_2H_4$ LUFO | 4.14 | 10.67 | 10.76 | 10.85 | 11.08 | 11.10 |

The relative amounts of ethylene → Cu and Cu → ethylene electron donation in each complex can be compared by examining the electron occupancy of the ethylene $\pi$-NBO and ethylene $\pi$*-NBO, respectively. Similar methodologies have been used successfully to study other metal–alkene adducts [52–55]. Table 4 contains selected data from the NBO calculations, with the orbital labels being derived from the major molecular orbital components of each particular NBO [31].

First examining the unligated cation **1**, the two principal donor → acceptor NBO interactions observed are the ethylene($\pi$) → Cu(4*s*) and the Cu(3*d*) → ethylene($\pi$*) interactions. The calculated occupancies of the ethylene $\pi$- and $\pi$*-orbitals are 1.779 and 0.085 electrons, respectively, indicating that 0.221 electrons are donated from the ethylene $\pi$-bonding orbital to the copper center (72%) while 0.085 electrons are delocalized from the copper to the ethylene $\pi$*-orbital (28%). The overall result of these two interactions is the net donation of 0.136 electrons from the coordinated ethylene to the copper(I) ion, yielding an ethylene molecule that is less electron rich than free ethylene. A natural atomic charge of 0.85 on the copper ion also indicates a net transfer of electron density to the copper center and consistent with previous reports that ethylene → Cu $\sigma$-donation of electron density is the dominant interaction in **1** [8–10]. Moreover, the combined donation of electron density to the ethylene $\pi$*-orbital and depletion of electron density from the ethylene $\pi$-orbital is consistent with the calculated lengthening of the C=C bond by ∼0.048 Å relative to free ethylene.

A similar analysis of complexes **2**–**6** reveals the impact of an electron-donating 1,10-phenanthroline ligand on the copper(I) center. Two dominant donor → acceptor NBO interactions observed in these complexes are again the ethylene($\pi$) → Cu(4*s*) and the Cu(3*d*) → ethylene($\pi$*) interactions. Additionally, the ethylene($\pi$) → Cu(4*p*) interaction is also predicted to play an important role in **2**–**6** (Fig. 5). The average electron occupancy of the ethylene $\pi$*-orbital in **2**–**6** is 0.225 electrons. This is larger than the occupancy of this orbital in **1** (0.085 electrons), indicating an increase in Cu → ethylene $\pi$-backbonding upon ligand coordination to the bare copper ion. However, the average occupancy of the ethylene $\pi$-orbital in **2**–**6** is 1.813 electrons, compared to 1.779 electrons in **1**, consistent with a decrease in ethylene → Cu donation in these complexes. Indeed, the Cu → ethylene $\pi$-backbonding interaction now dominates the electron donation in **2**–**6** (∼55%) while

**Table 4** Electron occupancies of selected natural bond orbitals (NBOs) for complexes **1**–**6**

| | **1** | **2** | **3** | **4** | **5** | **6** |
|---|---|---|---|---|---|---|
| $C_2H_4(\pi)$ | 1.77893 | 1.81416 | 1.81485 | 1.81495 | 1.81455 | 1.81578 |
| $C_2H_4(\pi^*)$ | 0.08536 | 0.21931 | 0.22180 | 0.22416 | 0.22996 | 0.23383 |

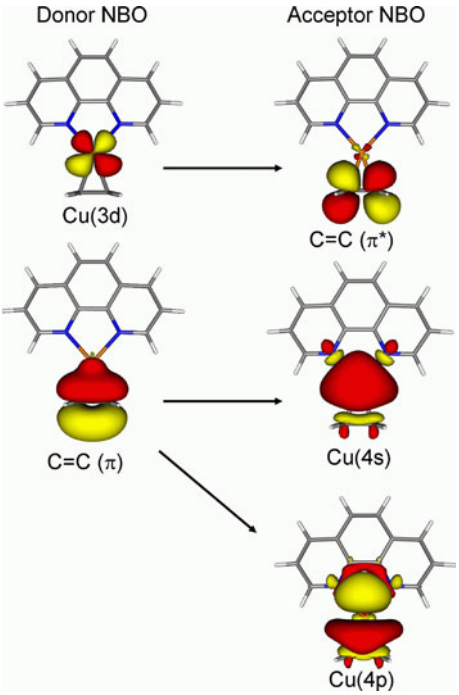


**Fig. 5** Selected donor–acceptor NBO interactions in [Cu(phen)($\eta^2$-$C_2H_4$)]$^+$

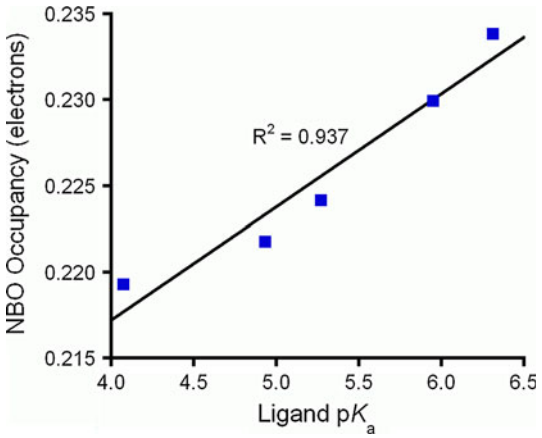


**Fig. 6** Electron occupancy of ethylene π*-NBO versus ligand p$K_a$ for complexes **2–6**

ethylene → Cu donation plays a lesser role (∼45%). This shift is similar to the effect reported for other copper(I)–alkene and alkyne complexes [26, 28]. Thus, the electron-donating 1,10-phenanthroline ligand increases the ability of the copper(I) center to donate electron density into the coordinated ethylene while decreasing the amount of ethylene → Cu donation. This yields an ethylene molecule that is more electron rich than free ethylene. Also, since population of the π*-orbital and depopulation of the π-bonding orbital both lead to lengthening of the ethylene C=C bond, the decrease in the depopulation of the ethylene π-orbital with ligand coordination would contribute to the relatively low degree of bond lengthening in **2–6** compared to **1**, even though population of the ethylene π*-orbital increases in **2–6**.

A similar analysis reveals the impact of systematically increasing ligand electron donor ability within the series **2–6.** As ligand basicity increases, the occupancy of the ethylene π*-orbital steadily increases from 0.219 to 0.234 electrons (Fig. 6). This slight but constant trend is consistent with an increase in the magnitude of Cu(3*d*) → ethylene(π*) backbonding and the MO analysis of these complexes. These results also support previous experimental and computational observations that increasing ligand basicity can enhance the ability of a copper(I) center to backbond with a coordinated alkene [5, 13, 26, 28]. These data are also in agreement with the predicted ethylene C=C bond lengths in **2–6** as well, with increasing π*-orbital occupancy leading to a longer C=C bond. Moreover, as seen in Table 4, the calculated electron occupancies of the ethylene π-orbital in **2–6** are approximately constant (∼1.814 to 1.815 electrons). Thus, increasing ligand basicity is predicted to have a smaller effect on the magnitude of ethylene(π) → Cu σ-donation.

### 3.4 ALMO-energy decomposition analysis (ALMO-EDA)

Energy decomposition analysis calculations were performed for complexes **1–6** utilizing the absolutely localized molecular orbital-energy decomposition analysis (ALMO-EDA) approach of Khaliullin et al. [32] as implemented in Q-Chem Version 3.2 [33]. This energy decomposition analysis allows for the determination of the interaction energies between two molecular fragments, which are the ethylene molecule and the [Cu(L)]$^+$ fragments for **2–6** and the ethylene molecule and the copper(I) ion for **1**. The ALMO-EDA has been successfully used to describe bonding interactions in other organometallic ethylene complexes such as [$PtCl_3(C_2H_4)$]$^-$ and is therefore useful for quantifying the binding interactions in **1–6** [32].

In the ALMO-EDA , the total binding energy ($\Delta E_{BIND}$) between the ethylene molecule and the [Cu(L)]$^+$ fragment can be divided into several contributions according to Eq. 1:

$$\Delta E_{BIND} = \Delta E_{FRZ} + \Delta E_{POL} + \Delta E_{CT} + \Delta E_{GD} \quad (1)$$

The first term, $\Delta E_{FRZ}$, is the SCF energy change for bringing the separately distorted ethylene and [Cu(L)]$^+$ fragments into the geometry of the complex without any relaxation of fragment MOs [32]. As such, $\Delta E_{FRZ}$ represents the sum of the Coulomb attraction and exchange–correlation repulsion between the ethylene molecule and the [Cu(L)]$^+$ fragment. The second term, $\Delta E_{POL}$, is a

polarization energy term that quantifies the energy lowering resulting from the intramolecular relaxation of the ethylene and $[Cu(L)]^+$ fragments' respective localized MOs in the field of the other fragment. $\Delta E_{CT}$ is the counterpoise corrected CT energy between the ethylene and $[Cu(L)]^+$ fragments. The CT energy is further divided into the ethylene → $[Cu(L)]^+$ component, the $[Cu(L)]^+$→ ethylene component, and higher-order (HO) relaxation effects [32]. Finally, $\Delta E_{GD}$ is the energetic change associated with distorting the isolated ethylene and $[Cu(L)]^+$ fragments from their individual optimized geometry to their geometry in the complex. The sum of these effects allow for the quantification of the total binding interactions between the ethylene molecule and each $[Cu(L)]^+$ fragment.

Table 5 lists the results of the ALMO-EDA calculations for complexes **1**–**6**. For the unligated **1**, the total calculated copper(I)–ethylene binding energy is −207.4 kJ/mol. This is comparable to the value obtained by Hertwig and co-workers using the related Morokuma Bond Decomposition analysis method ($\Delta E_{BIND} = -216.7$ kJ/mol) [8] and compares to the experimentally reported value of the $[Cu]^+$–$(C_2H_4)$ bond dissociation energy of 173.6 kJ/mol [8]. The value of $\Delta E_{FRZ}$ is small and slightly repulsive (+35.2 kJ/mol). The energetic penalty for geometric distortion is also small (+17.6 kJ/mol). Favorable polarization effects between the copper(I) cation and the ethylene molecule ($\Delta E_{POL} = -111.7$ kJ/mol) provide a major contribution to the total binding energy. Of the CT terms, the ethylene → Cu donation accounts for the majority of the stabilization (−91.1 kJ/mol), while the Cu → ethylene backdonation accounts for −44.1 kJ/mole, and the higher-order CT for −13.3 kJ/mole. Thus, of the two main CT terms, ethylene → Cu CT accounts for ∼67% of the total amount, and the Cu → ethylene CT accounts for ∼33%. These results are consistent with the findings of Hertwig and co-workers [8] and with the NBO calculations in this study for **1** which show that ethylene → copper donation is the dominant CT term in $[Cu(C_2H_4)]^+$.

As observed in the NBO calculations, the impact of adding an electron-donating ligand to the copper center is important. The average calculated binding energy between ethylene and the $[Cu(L)]^+$ fragments in **2**–**6** is −146.4 kJ/mol. These values are ∼60 kJ/mol less favorable than that calculated for **1** (−207.5 kJ/mol), suggesting a significantly weaker copper(I)–ethylene interaction in the presence of the 1,10-phenanthroline ligands. This decrease in binding energy is largely the result of non-CT effects; $\Delta E_{FRZ}$ is ∼30 kJ/mole more repulsive in complexes **2**–**6** than in **1**, accounting for approximately half of the decrease in binding energy. Similarly, favorable polarization effects ($\Delta E_{POL}$) also decrease by ∼35 kJ/mole in complexes **2**–**6** relative to **1**. Thus, addition of an electron-donating ligand results in the loss of ∼65 kJ/mol of favorable non-CT terms.

Consistent with the NBO results, the average amount of Cu → ethylene CT stabilization for **2**–**6** (−98.5 kJ/mol) is significantly larger than that for **1** (−44.1 kJ/mol), supporting the premise that electron-donating ligands enhance the ability of the copper(I) ion to backbond with the ethylene molecule. Similarly, the average amount of ethylene → Cu CT in **2**–**6** (−57.6 kJ/mol) is predicted to be significantly less than that for **1** (−91.1 kJ/mol) Coordination of an electron-donating 1,10-phenanthroline ligand is therefore predicted to make the copper(I) center both more able to donate electron density into the empty $\pi^*$-orbital of the ethylene molecule and less able to accept electron density from the filled $\pi$-orbital of the ethylene.

It is also useful to compare the effects of increasing ligand basicity within the series of complexes **2**–**6**. $\Delta E_{FRZ}$ increases from 64.7 kJ/mol for **2** to 70.9 kJ/mol for **6**, consistent with a less attractive interaction between the positively charged copper ion and the ethylene molecule as ligand donor ability increases (Fig. 7). Similarly, favorable polarization effects ($\Delta E_{POL}$) (Fig. 8) and ethylene → Cu CT decrease over the same series. In contrast, favorable Cu → ethylene CT is predicted to steadily increase as ligand p$K_a$ increases (Fig. 9). These results are again in

**Table 5** ALMO-EDA of $[Cu(L)(\eta^2\text{-}C_2H_4)]^+$ complexes **1**–**6** (energies in kJ/mol)

| | **1** | **2** | **3** | **4** | **5** | **6** |
|---|---|---|---|---|---|---|
| Ligand p$K_a$ | NA | 4.07 | 4.93 | 5.27 | 5.95 | 6.31 |
| $\Delta E_{FRZ}$ | 35.212 | 64.714 | 66.605 | 66.655 | 67.897 | 70.910 |
| $\Delta E_{POL}$ | −111.700 | −71.665 | −71.278 | −71.233 | −70.523 | −70.265 |
| $\Delta E_{CT}$ (Cu → eth) | −44.099 | −94.996 | −96.316 | −97.567 | −100.724 | −102.652 |
| $\Delta E_{CT}$ (eth → Cu) | −91.066 | −57.965 | −57.681 | −57.636 | −57.570 | −57.219 |
| $\Delta E_{CT}$ (HO) | −13.349 | −9.053 | −8.877 | −8.663 | −8.548 | −8.290 |
| $\Delta E_{GD}$ ($[Cu(L)]^+$) | 0.000 | 3.409 | 4.279 | 4.321 | 4.298 | 4.684 |
| $\Delta E_{GD}$ (eth) | 17.553 | 17.392 | 17.533 | 17.747 | 18.144 | 18.194 |
| $\Delta E_{BIND}$ | −207.449 | −148.165 | −145.735 | −146.377 | −147.026 | −144.639 |

agreement with the NBO calculations. In summary, the ALMO-EDA calculations predict that while favorable Cu → ethylene CT stabilization increases with ligand basicity, a simultaneous decrease in favorable ethylene → Cu CT and a decrease in favorable non-CT contributions is also observed. Thus, the overall calculated binding energies are relatively similar for the different $[Cu(L)(C_2H_4)]^+$ complexes (−144.6 to −148.2 kJ/mole) and while there are strong correlations between ligand p$K_a$ and the individual components of the copper–ethylene interaction, changes in favorable and unfavorable effects largely cancel out.

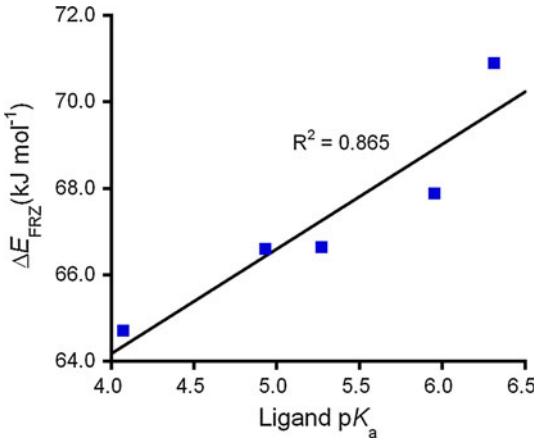


**Fig. 7** $\Delta E_{FRZ}$ versus ligand p$K_a$ for complexes **2–6**

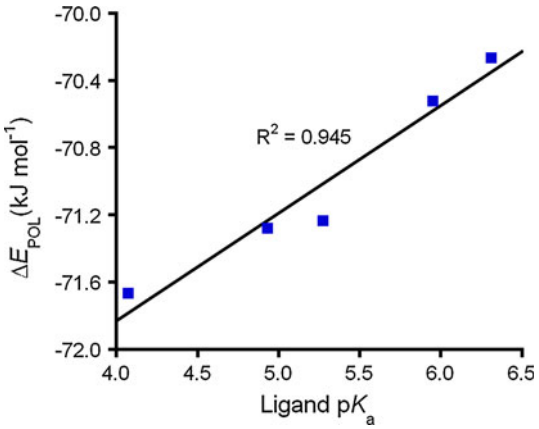


**Fig. 8** $\Delta E_{POL}$ versus ligand p$K_a$ for complexes **2–6**

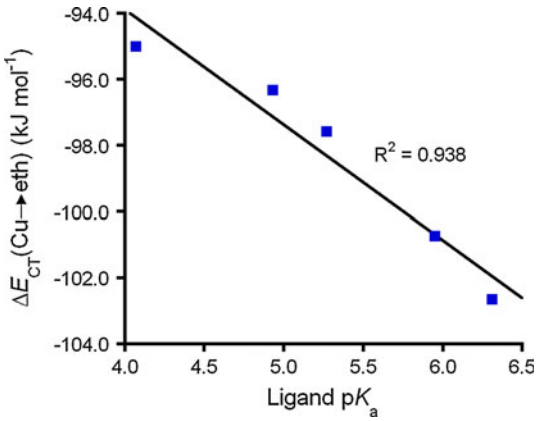


**Fig. 9** $\Delta E_{CT}$ (Cu → eth) versus ligand p$K_a$ for complexes **2–6**

### 3.5 Calculated free energies of binding

The experimentally observed linear relationship between the formation constant of the $[Cu(L)(\eta^2\text{-}C_2H_4)]^+$ complexes from $[Cu(L)(NCCH_3)_n]^+$ and the p$K_a$ of the bidentate 1,10-phenanthroline ligands was originally attributed primarily to the increased backbonding ability of the copper center [16, 17]. However, despite predicting an increase in Cu → ethylene CT with increasing ligand basicity, the ALMO-EDA calculations predict no significant changes or trends in overall copper(I)–ethylene binding energy with changing ligand basicity due to simultaneous unfavorable changes frozen density and polarization terms. To help understand the reported experimentally observed linear relationship between ligand basicity and the formation constant of the $[Cu(L)(\eta^2\text{-}C_2H_4)]^+$ complexes, the free energy of formation of these complexes from $[Cu(L)(NCCH_3)_n]^+$ precursors was examined. While the identity

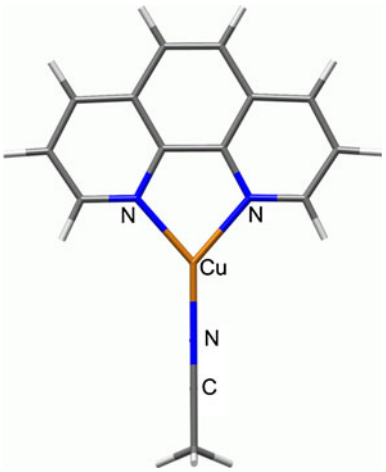


**Fig. 10** Optimized geometry of $[Cu(phen)(NCCH_3)]^+$

**Table 6** Calculated $\Delta G$ for displacement of acetonitrile by ethylene in $[Cu(L)(NCCH_3)]^+$ complexes (energy in kJ/mol)

| Ligand | $\Delta G_{gas}$ | $\Delta G_{MeOH}$ |
|---|---|---|
| Cl–phen | 34.86 | −0.06 |
| Phen | 33.82 | −0.90 |
| Me–phen | 32.78 | −1.17 |
| $Me_2$–phen | 30.85 | −1.92 |
| $Me_4$–phen | 28.95 | −1.73 |

of the starting copper(I) species was not specifically identified in the original experimental studies [16, 17] and a number of possible species could be proposed, we have chosen to examine the putative monoacetonitrile adducts $[Cu(L)(NCCH_3)]^+$ [where L = Cl-phen (**8**), phen (**9**), Me-phen (**10**), $Me_2$-phen (**11**), and $Me_4$-phen (**12**)] as a potential starting complexes for comparing the impact of ligand basicity in these ligand exchange reactions (Eq. 2).

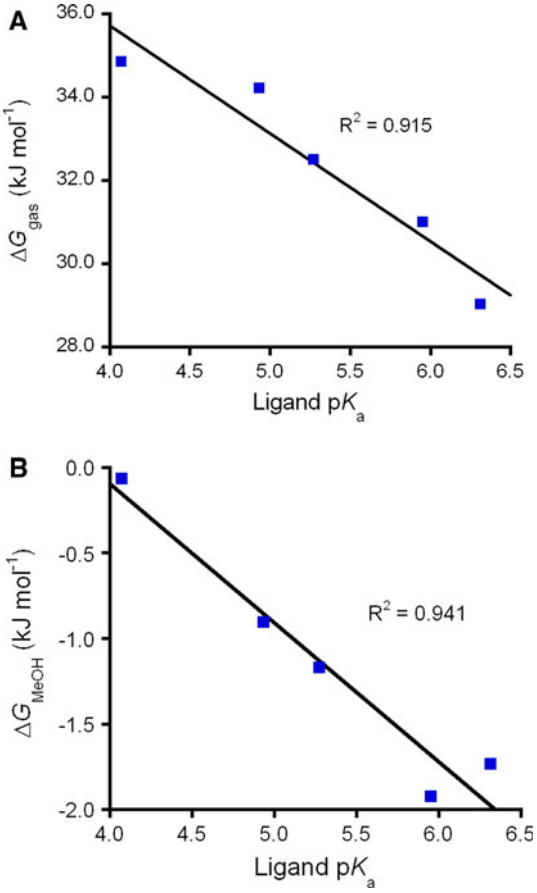


**Fig. 11** Calculated $\Delta G$ for the displacement of MeCN by ethylene versus ligand p$K_a$ in the gas phase (**a**) and in methanol solvent (**b**)

$$[Cu(L)(NCCH_3)]^+ + C_2H_4 \rightleftarrows [Cu(L)(C_2H_4)]^+ + CH_3CN \quad (2)$$

Figure 10 shows the geometry optimized structure of $[Cu(phen)(NCCH_3)]^+$ (**9**) as a representative example of these starting complexes. Single-point energy calculations for all species were performed in the gas phase and, for comparison, in methanol solvent utilizing the CPCM solvation model [44]. The values for these calculated changes in free energy are listed in Table 6. Figure 11a, b show plots of the calculated free energy changes of the reaction versus the p$K_a$ of the 1,10-phenanthroline ligands in the gas phase and MeOH, respectively. As can be observed, increasing the electron-donating strength of the supporting ligand generally results an increasingly favorable displacement of acetonitrile by ethylene, both in the gas phase and in solvent. This is consistent with the experimentally observed trend in the binding constant for $[Cu(L)(\eta^2\text{-}C_2H_4)]^+$ complexes, while the reaction becomes more favorable in the polar medium.

ALMO-EDA calculations were similarly performed on the $[Cu(L)(NCCH_3)]^+$ complexes **8**–**12** to determine the impact of ligand basicity on overall $[Cu(L)]^+$–$(NCCH_3)$ binding energy. As seen in Table 7, the total calculated binding energy of the acetonitrile molecule to the $[Cu(L)]^+$ fragment decreases by 7.1 kJ/mol with increasing ligand basicity across the series (Fig. 12). Because acetonitrile is predominantly a $\sigma$-donor ligand and a relatively poor $\pi$-acid compared to ethylene, increasing ligand basicity only provides ~2.1 kJ/mol of additional stabilization in terms of $[Cu(L)]^+ \rightarrow (NCCH_3)$ CT, compared to 7.7 kJ/mole for ethylene. Non-CT $[Cu(L)]^+$–$(NCCH_3)$ interactions become significantly less favorable, however, as ligand basicity increases. $\Delta E_{FROZ}$ becomes less favorable by 6.7 kJ/mol and $\Delta E_{POL}$ simultaneously becomes less favorable by 2.0 kJ/mol. Thus, the decrease in non-CT stabilization outweighs the increase in favorable CT contributions, yielding an overall decrease in the $[Cu(L)]^+$–$(NCCH_3)$

**Table 7** ALMO-EDA of $[Cu(L)(NCCH_3)]^+$ complexes **8**–**12** (energies in kJ/mol)

| | **8** | **9** | **10** | **11** | **12** |
|---|---|---|---|---|---|
| Ligand p$K_a$ | 4.07 | 4.93 | 5.27 | 5.95 | 6.31 |
| $\Delta E_{FRZ}$ | −9.729 | −6.213 | −6.842 | −6.123 | −3.062 |
| $\Delta E_{POL}$ | −88.781 | −88.156 | −87.903 | −87.121 | −86.751 |
| $\Delta E_{CT}$ (Cu → $NCCH_3$) | −29.565 | −29.948 | −30.278 | −31.106 | −31.657 |
| $\Delta E_{CT}$ ($NCCH_3$ → Cu) | −41.763 | −41.388 | −41.314 | −41.172 | −40.745 |
| $\Delta E_{CT}$ (HO) | −5.747 | −5.784 | −5.862 | −5.950 | −6.005 |
| $\Delta E_{GD}$ ($[Cu(L)]^+$) | 6.619 | 5.425 | 6.999 | 7.357 | 6.319 |
| $\Delta E_{GD}$ ($NCCH_3$) | −0.206 | −0.207 | −0.205 | −0.202 | −0.200 |
| $\Delta E_{BIND}$ | −169.172 | −166.271 | −165.403 | −164.318 | −162.101 |
| $\Delta\Delta E_{BIND}$ (eth–$NCCH_3$) | 21.007 | 20.536 | 19.026 | 17.292 | 17.462 |

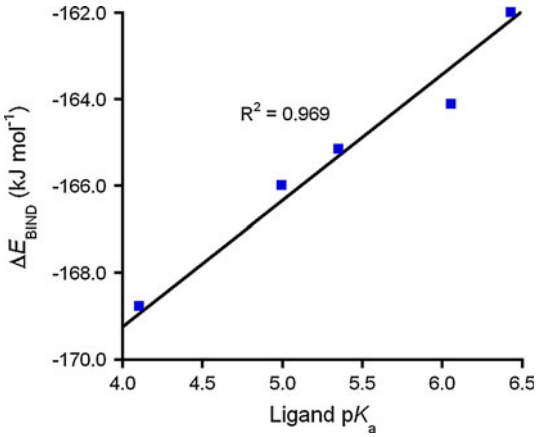


**Fig. 12** Binding energy of $NCCH_3$ to $[Cu(L)]^+$ versus ligand p$K_a$ for complexes **8**–**12**

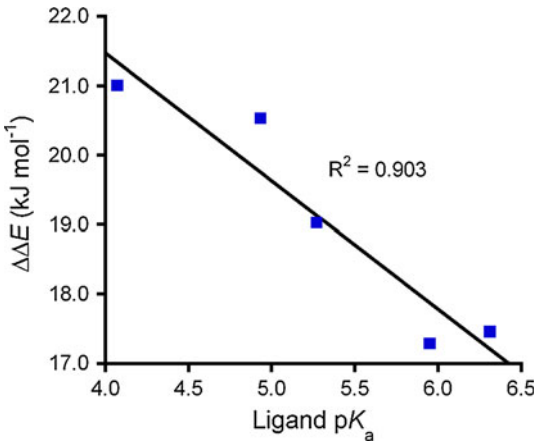


**Fig. 13** Difference in binding energy of $C_2H_4$ and $NCCH_3$ to $[Cu(L)]^+$ ($\Delta\Delta E_{BIND}$) versus ligand p$K_a$

binding energy. This in turn increases the favorability of acetonitrile dissociation with more basic ligands. Comparing the differences in binding energies of ethylene and acetonitrile to the $[Cu(L)]^+$ fragments [$\Delta\Delta E_{BIND} = \Delta E_{BIND}(C_2H_4) - \Delta E_{BIND}(NCCH_3)$], a correlation is observed with ligand p$K_a$, consistent with the free energy calculations (Table 7; Fig. 13). Thus, while increasing the electron-donating ability of the 1,10-phenanthroline ligand results in relatively small net change in the $[Cu(L)]^+$–$(C_2H_4)$ binding energy, there is a clear decrease in the binding energy of the acetonitrile molecule with more strongly donating ligands which could lead to a more favorable displacement of acetonitrile with ethylene for more strongly donating ligands.

## 4 Conclusion

DFT calculations have been used to determine the impact of the presence of an ancillary ligand and the basicity of such a ligand on the binding interactions between the copper(I) ion and the ethylene molecule. While Cu → ethylene $\pi$-backbonding and its dependence on an ancillary ligand is often the main focus of the study of copper(I)–ethylene adducts, these calculations demonstrate the complex nature of these binding interactions and show how CT and non-CT components are all directly affected by the presence of an ancillary ligand and the basicity of that ligand.

Consistent with previous reports, both NBO and ALMO-EDA calculations suggest that ethylene → copper CT is the dominant CT in $[Cu(C_2H_4)]^+$ (~70%), with Cu → ethylene CT playing the lesser role (~30%). Molecular orbital analysis reveals that this is primarily the result of a low degree of interaction between the low energy Cu(3*d*) orbitals (−15.7 eV) and the empty $\pi$*-orbital of the ethylene molecule (−0.2 eV). Moreover, ALMO-EDA calculations reveal that favorable polarization effects and a small frozen density repulsion term provide a substantial contribution to the overall binding energy between the two fragments.

Addition of a 1,10-phenanthroline ligand to the copper center has a dramatic effect on the nature of the binding interactions. NBO and ALMO-EDA calculations both suggest an increase in the magnitude of Cu → ethylene CT upon coordination of the electron-donating ligands when compared to the bare $[Cu(C_2H_4)]^+$ cation. Indeed, NBO and ALMO-EDA calculations reveal that Cu → ethylene CT in the $[Cu(L)(C_2H_4)]^+$ complexes contributes the majority of CT stabilization, with ethylene → copper donation providing the lesser amount. Molecular orbital analysis suggests that the increase in Cu → ethylene CT is a result of the higher energy Cu(3*d*)-HOFO of the $[Cu(L)]^+$ fragment (ca −10 eV), which interacts more with the empty $\pi$*-orbital of the ethylene molecule. Moreover, as ligand basicity increases, the energy of the Cu(3*d*)-HOFO steadily increases, as does mixing with the empty ethylene $\pi$*-orbital, consistent with a direct increase in Cu → ethylene $\pi$-backbonding. However, while CT stabilization is predicted to steadily increase with increasing ligand basicity, polarization and frozen density terms simultaneously become less favorable. Thus, while all CT and non-CT components of the $[Cu(L)]^+$–$(C_2H_4)$ binding energy are strongly correlated with the p$K_a$ of the 1,10-phenanthroline ligands, the overall binding energy changes little and displays no clear trend due to the complex nature of the interactions.

Despite the predictions of little change in $[Cu(L)]^+$–$(C_2H_4)$ binding energy, calculated free energy changes for the displacement of acetonitrile by ethylene from the putative $[Cu(L)(CH_3CN)]^+$ complexes show a good correlation with ligand p$K_a$, with ethylene binding becoming more favorable with increasing ligand basicity. ALMO-EDA calculations reveal that $[Cu(L)]^+$−$(NCCH_3)$ binding energy decreases significantly with increasing ligand p$K_a$

due largely to less favorable polarization and a more repulsive frozen density term. Thus, while $[Cu(L)]^+$–$(C_2H_4)$ binding energy remains relatively constant, the decrease in $[Cu(L)]^+$–$(CH_3CN)$ binding energy with increasing ligand basicity can potentially help to explain the experimentally observed preference for ethylene binding with more strongly donating ligands in synthetic systems.

**Acknowledgments** Acknowledgment is made to the Donors of the American Chemical Society Petroleum Research Fund (Grant 42303-GB3) and to Stetson University for financial support of this research.

## References

1. Rodriguez FI, Esch JJ, Hall AE, Binder BM, Schaller GE, Bleecker AB (1999) Science 283:996
2. Pirrung MC, Bleecker AB, Inoue Y, Rodriguez FI, Sugaware N, Wada T, Zou Y, Binder BM (2008) Chem Biol 15:313
3. Straub BF, Gruber I, Rominger F, Hofmann P (2003) J Organomet Chem 684:124
4. Brandt P, Sodergren MJ, Andersson PG, Norrby P-O (2000) J Am Chem Soc 122:8013
5. Wang X-S, Zhao H, Li Y-H, Xiong R-G, You X-Z (2005) Top Catal 35:43
6. Green O, Bhavesh AG, Burstyn JN (2009) Inorg Chem 48:5704
7. Ziegler T, Rauk A (1979) Inorg Chem 18:1558
8. Hertwig RH, Koch W, Schroder D, Schwarz H, Hrusak J, Schwerdtfeger P (1996) J Phys Chem 100:12253
9. Bohme M, Wagener T, Frenking G (1996) J Organomet Chem 520:31
10. Nechaev MS, Rayon VM, Frenking G (2004) J Phys Chem A 108:3134
11. Allen JJ, Barron AR (2009) Dalton Trans 878
12. Mingos DMP (2001) J Organomet Chem 635:1
13. Dias HVR, Wu J (2008) Eur J Inorg Chem 509
14. Hirsch J, DeBeer George S, Solomon EI, Hedman B, Hodgson KO, Burstyn JN (2001) Inorg Chem 40:2439
15. Suenaga Y, Wu LP, Kuroda-Sowa T, Munakata M, Maekawa M (1997) Polyhedron 16:67
16. Munakata M, Kitagawa S, Kosome S, Asahara A (1986) Inorg Chem 25:2622
17. Masuda H, Yamamoto N, Taga T, Machida K, Kitagawa S, Munakata MJ (1987) J Organomet Chem 322:121
18. Thompson JS, Harlow RL, Whitney JF (1983) J Am Chem Soc 105:3522
19. Dias HVR, Lu H-L, Kim H-J, Polach SA, Goh TKHH, Browning RG, Lovely CJ (2002) Organometallics 21:1466
20. Dias HVR, Wang X, Diyabalanage HVK (2005) Inorg Chem 44:7322
21. Dai X, Warren TW (2001) Chem Commun 1998
22. Straub BF, Eisentrager F, Hofmann P (1999) Chem Commun 2507
23. Gasque L, Medina G, Ruiz-Ramírez L, Moreno-Esparza R (1999) Inorg Chim Acta 288:106
24. Laitar DS, Mathison JN, Davis WM, Sadighi JP (2003) Inorg Chem 42:7354
25. Hill LRM, Gherman BF, Aboelella NW, Cramer CJ, Tolman WB (2006) Dalton Trans 4944
26. Srebro M, Mitoraj M (2009) Organometallics 28:3650
27. Thompson JS, Bradley AZ, Park K-H, Dobbs KD, Marshall W (2006) Organometallics 25:2712
28. Oguadinma PO, Schaper F (2009) Organometallics 28:6721
29. Gorelsky SI, Lever ABP (2001) J Organomet Chem 635:187
30. Gorelsky SI (1997) AOMix: program for molecular orbital analysis. York University, Toronto
31. Reed AE, Weinhold FJ (1985) Chem Phys 83:1736
32. Khaliullin RZ, Cobar EA, Lochan RC, Bell AT, Head-Gordon MJ (2007) Phys Chem A 111:8753
33. Shao Y, Fusti-Molnar L, Jung Y, Kussmann J, Ochsenfeld C, Brown ST, Gilbert ATB, Slipchenko LV, Levchenko SV, O'Neill DP, DiStasio RA Jr, Lochan RC, Wang T, Beran GJO, Besley NA, Herbert JM, Lin CY, Voorhis TV, Chien SH, Sodt A, Steele RP, Rassolov VA, Maslen PA, Korambath PP, Adamson RD, Austin B, Baker J, Byrd EFC, Daschel H, Doerksen RJ, Dreuw A, Dunietz BD, Dutoi AD, Furlani TR, Gwaltney SR, Heyden A, Hirata S, Hsu S-P, Kedziora G, Khaliullin RZ, Klunzinger P, Lee AM, Lee MS, Liang WZ, Rosta E, Sherrill CD, Simmonett AC, Subotnik JE, Woodcock III HL, Zhang W, Bell AT, Chakraborty AK, Chipman DM, Keil FJ, Warshel A, Hehre WJ, Schaefer III HF, Kong J, Krylov AI, Gill PMW, Head-Gordon M (2006) Phys Chem Chem Phys 8:317
34. Becke AD (1998) Phys Rev A 38:3098
35. Becke AD (1993) J Chem Phys 98:5648
36. Lee CT, Yang WT, Parr RG (1988) Phys Rev B 37:785
37. Frisch MJ, Trucks GW, Schlegel HB, Scuseria GE, Robb MA, Cheeseman JR, Montgomery JA Jr, Vreven T, Kudin KN, Burant JC, Millam JM, Iyengar SS, Tomasi J, Barone V, Mennucci B, Cossi M, Scalmani G, Rega N, Petersson GA, Nakatsuji H, Hada M, Ehara M, Toyota K, Fukuda R, Hasegawa J, Ishida M, Nakajima T, Honda Y, Kitao O, Nakai H, Klene M., Li X, Knox JE, Hratchian HP, Cross JB, Adamo C, Jaramillo J, Gomperts R, Stratmann RE, Yazyev O, Austin AJ, Cammi R, Pomelli C, Ochterski JW, Ayala PY, Morokuma K, Voth GA, Salvador P, Dannenberg JJ, Zakrzewski VG, Dapprich S, Daniels AD, Strain MC, Farkas O, Malick DK, Rabuck AD, Raghavachari K, Foresman JB, Ortiz JV, Cui Q, Baboul AG, Clifford S, Cioslowski J, Stefanov BB, Liu G, Liashenko A, Piskorz P, Komaromi I, Martin RL, Fox DJ, Keith T, Al-Laham MA, Peng CY, Nanayakkara A, Challacombe M, Gill PMW, Johnson B, Chen W, Wong MW, Gonzalez C, Pople JA (2004) Gaussian 03; Revision E.01. Gaussian, Inc., Wallingford
38. Dolg M, Wedig U, Stoll H, Preuss H (1987) J Chem Phys 86:866
39. Hehre WJ, Ditchfield R, Pople JA (1972) J Chem Phys 56:2257
40. Francl MM, Pietro WJ, Hehre WJ, Binkley JS, Gordon MS, Defrees DJ, Pople JA (1982) J Chem Phys 77:3654
41. Heppner DE, Gherman BF, Tolman WB, Cramer CJ (2006) Dalton Trans 4773
42. Dai X, Warren TH (2004) J Am Chem Soc 126:10085
43. Krishnan R, Binkley JS, Seeger R, Pople JA (1980) J Chem Phys 72:650
44. Barone V, Cossi M (1998) J Phys Chem A 102:1995
45. Scott AP, Radom L (1996) J Phys Chem 100:16502
46. Bartell LS, Roth CD, Hollowell KK, Young JE Jr (1965) J Chem Phys 42:2683
47. Cheng P-T, Cook CD, Nyburg SC, Wan KY (1971) Inorg Chem 10:2210
48. Cheng P-T, Nuburg SC (1972) Can J Chem 50:912
49. Dreissig W, Dietrich H (1981) Acta Cryst B37:931
50. Gorelsky SI, Lever ABP (2001) J Organomet Chem 635:187
51. Rusanova J, Rusanov E, Gorelsky SI, Christendat D, Popescu R, Farah AA, Beaulac R, Reber C, Lever ABP (2006) Inorg Chem 45:6246
52. Cedeno DL, Sniatynsky R (2005) Organometallics 24:3882
53. Schlappi DN, Cedeno DL (2003) J Phys Chem A 107:8763
54. Ikeda A, Nakao Y, Sato H, Sakaki S (2007) J Phys Chem A 111:712
55. Uddin J, Dapprich S, Frenking G, Yates BF (1998) Organometallics 18:457